EARTH SURFACE PROCESSES AND LANDFORMS
Earth Surf. Process. Landforms **44**, 681–698 (2019)

Published online 26 November 2018 in Wiley Online Library
(wileyonlinelibrary.com) DOI: 10.1002/esp.4523

Intertidal boulder transport: A proposed methodology adopting Radio Frequency Identification (RFID) technology to quantify storm induced boulder mobility

Linley John Hastewell,* Martin Schaefer, Malcolm Bray and Robert Inkpen
Department of Geography, University of Portsmouth, Portsmouth, UK

Received 15 January 2018; Revised 27 September 2018; Accepted 27 September 2018

*Correspondence to: Linley John Hastewell, Department of Geography, University of Portsmouth, Portsmouth, PO1 3HE, UK. E-mail: linley.hastewell@port.ac.uk

ESPL
Earth Surface Processes and Landforms

ABSTRACT: Boulder transport is an area of growing interest to coastal scientists as a means of improving our understanding of the complex interactions between extreme wave activity and the evolution of rocky coasts. However, our knowledge of the response of intertidal boulder deposits to contemporary storm events remains limited due to a lack of quantifiable field-based evidence.

We address this by presenting a methodology incorporating Radio Frequency Identification (RFID) tagging and Differential Global Positioning Navigation Satellite System (DGNSS) technology to monitor and accurately quantify the displacement of RFID tagged boulders resulting from storm wave activity. Based on preliminary findings we highlight the suitability of the technology and methodology to better understand the spatial and temporal response of intertidal boulders to contemporary storm events.

We inserted RFID tags in 104 limestone boulders (intermediate axes from 0.27 to 2.85 m) across a range of morphogenic settings at two sites on the intertidal shore platforms at Bembridge, Isle of Wight (UK). Fifteen topographic surveys were conducted between July 2015 and May 2017 to relocate and record tagged boulder locations (tag recovery rate: 91%). The relocated boulder coordinate data from both sites identified 164 individual transport events in 63% of the tagged boulder array amounting to 184.6 m of transport, including the displacement of a boulder weighing more than 10 tonnes.

Incidents of boulder quarrying and overturning during transport were also recorded, demonstrating that despite the relatively sheltered location, intertidal boulders are created and regularly transported under moderate storm conditions. This suggests that contemporary storm events have a greater propensity to mobilise boulders in the intertidal range than has previously been realised.

Consequently, by documenting our methodology we provide guidance to others and promote further use of RFID technology to enable new hypotheses on boulder transport to be tested in a range of field settings and wave regimes. © 2018 John Wiley & Sons, Ltd.

KEYWORDS: RFID tagging; boulder transport; storm events; sediment tracing; coastal change

Introduction

The anticipated increase in storm activity and intensity resulting from climate change (Easterling *et al.,* 2000; Beniston *et al.,* 2007) is expected to drive geomorphic alteration to shore platforms and increase the vulnerability of coastal zones globally (Paris *et al.,* 2011). Given the irreversible erosional impact of storm waves on rocky coasts (Naylor *et al.,* 2010) understanding the geomorphic response to such events is of growing significance. As a result, storm wave impacts on rocky coasts are of increasing interest in terms of understanding landform evolution and monitoring coastal change.

The presence of large boulders on shore platforms is testament to the dynamic nature of the coastal environment. However, the mechanisms that facilitate detachment, transport and deposition of boulder-sized sediment within the intertidal zone are poorly understood. We defined boulders as clasts with an intermediate (*I*) axis between 0.25 and 4.1 m (Blair and McPherson, 1999).

Sediment tracing provides a means of monitoring and quantifying displacement while offering an insight to the hydrodynamic conditions that enable episodes of mobility (Lee *et al.,* 2000; Sear *et al.,* 2000). The basic principle of sediment tracing is to introduce material to a study site which is distinct from, yet accurately reflects the physical properties (e.g. particle size, shape and density) of the indigenous sediment (Sear *et al.,* 2000; Black *et al.,* 2007; Lee *et al.,* 2007). This can be achieved using artificial tracers such as aluminium cast material (Bray *et al.,* 1996) or by adapting the indigenous material found at the selected study site. Following tracer deployment, successive searches are undertaken to recover the particles and record their precise location allowing distance, direction and frequency of transport to be determined.

In littoral settings sediment tracers are monitored *in situ* where they are subjected to a series of site specific conditions (e.g. wave climate, tidal regime, topography and bathymetry) which are difficult, if not impossible to accurately replicate within the confines of the laboratory. This paper demonstrates the feasibility of using radio frequency identification (RFID) technology in combination with periodic topographic surveys using a differential global positioning navigation satellite system (DGNSS) to accurately quantify the mobility of intertidal boulders resulting from contemporary storm activity.

Historically, tracer techniques have included painted sediment (Russell, 1960**;** Jolliffe, 1964**;** Nordstrom and Jackson, 1993); radioisotopic tracers (Steers and Smith, 1956; Kidson *et al.,* 1958), magnetic tracers (Osborne, 2005), aluminium tracers (Wright *et al.,* 1978), electronic radio transmitters (Bray *et al.,* 1996) and RFIDs (Dickson *et al.,* 2011; Dolphin *et al.,* 2016) as a means of monitoring littoral sediment transport across a range of particle sizes. The development of tracer techniques has been driven by the need to improve tracer recovery rates over broader timescales. Table I identifies how different tracer methods and technological advances have facilitated this. It also highlights the preponderance of research focusing on pebble and cobble-sized particles, and subsequently, the paucity of long-term tracer studies relating specifically to the mobility of boulder-sized clasts. Further reviews pertaining to the development of sediment tracing techniques have been published by Sear *et al.* (2000) and Chapuis *et al.* (2014).

RFID tagging has proven to be effective in transport studies in both fluvial (Liébault *et al.,* 2012; Nathan Bradley and Tucker, 2012) and littoral settings (Allan *et al.,* 2006; Dickson *et al.,* 2011; Dolphin *et al.,* 2016). It has facilitated longer term monitoring studies yielding more favourable recovery rates when compared with alternative methods. The success of previous RFID-based studies documenting sediment transport was integral to our decision to adopt this technology for monitoring boulder displacement.

It is well documented that storm waves have the ability to detach, transport and deposit boulders on intertidal shore platforms (Barbano *et al.,* 2010; Etienne and Paris, 2010; Goto *et al.,* 2011; Paris *et al.,* 2011; Shah-hosseini *et al.,* 2011; Stephenson and Naylor, 2011; Cox *et al.,* 2012; Biolchi *et al.,* 2016). Boulder accumulations on shore platforms frequently develop distinctive geomorphic features such as clusters, ridges, fields and cliff top deposits (Nott, 2003a; Paris *et al.,* 2011). These boulder assemblages have been used to infer the mechanisms by which detachment, transport and emplacement occur, including past tsunamigenic wave events (Etienne *et al.,* 2011; Engel and May, 2012; Goto *et al.,* 2012; Nandasena *et al.,* 2013; Mottershead *et al.,* 2014) and contemporary storm activity (Fichaut and Suanez, 2011; Hall, 2011; Autret *et al.,* 2016; Cox *et al.,* 2018). However, despite growing interest in the effects of extreme waves the subsequent modes and rates of boulder transport over time are poorly understood owing to a lack of accurate, reliable and quantifiable field data (Goto *et al.,* 2011; Paris *et al.,* 2011; Moses, 2014).

Recent studies have sought to address this by documenting boulder transport during, and resulting from, contemporary storm events. Extreme storm activity occurred in the winter of 2013–2014 which had a dramatic impact on the Atlantic coastline of Europe (Masselink *et al.,* 2016a) with reports of significant wave heights exceeding 9 m (Castelle *et al.,* 2015). During this period Autret *et al.* (2016) recorded the morphological and sedimentological alteration of cliff-top boulder deposits. They documented quarrying of 178 clasts, one weighing 86 tonnes, and the transport of 507 blocks some as far as 40 m inland at elevations up to 14 m above mean sea level. This was achieved using unmanned aerial vehicles (UAVs) and kite-mounted cameras which were deployed to obtain pre/post site imagery for comparative purposes. These techniques were complimented by field observations of boulder mobility and the use of pressure sensors to establish hydrodynamic conditions during the period of storm activity.

Table I. Littoral tracer studies of coarse sediment reporting the selected tracer technique, duration of study and rate of recovery

Authors & date	Tracer method/technique	Particle size (after Blair and McPherson, 1999)	No. of deployed tracers	Study duration	Reported recovery rate
Kidson *et al.,* 1958	Radioactive	Size not specified - pebbles	2000	6 weeks	~5%
Jolliffe, 1964	Artificial (concrete) and painted	Coarse pebbles/fine cobbles	2500	4.5 days	58%
Nordstrom and Jackson, 1993	Painted	Fine/coarse pebbles	8.9 kg	29 days	6% (0.53 kg)
Ciavola and Castiglione, 2009	Painted	Cobbles (>64 mm)	35.1 kg	4 days	30% (10.5 kg)
Naylor *et al.,* 2016	Painted and numbered	Coarse cobbles - fine/medium boulders	48	4 days	81%
Wright *et al.,* 1978	Aluminium	Very coarse pebbles	75	17 days	61%
Bray *et al.,* 1996	Aluminium & Electronic	34–65 mm: very coarse pebbles	246 and 139 respectively	6 weeks	47–96% and 80–100% respectively
Osborne, 2005	Magnetic	Intermediate axis between 19 and 108 mm: coarse pebbles/fine cobbles	90	2 months	93%
Allan *et al.,* 2006	RFID	Mode value 90.5 mm: fine cobbles	400	17 months	90% after 8 months 18% after 17 months
Curtiss *et al.,* 2009	RFID	23 mm: coarse pebbles	96	14 months	>80% throughout survey
Dickson *et al.,* 2011	RFID	Minimum long and short axes of 60 mm and 30 mm respectively	180	8 months	0–30%
Miller and Warrick, 2012	RFID	64–128 mm: fine cobbles	54	24 hours	93–100%
Dolphin *et al.,* 2016	RFID	Size not specified: gravel	940	3 years	78% on completion
Han *et al.,* 2017	RFID	64 mm: very coarse pebbles/fine cobbles	200	2 days	33%

Stephenson and Naylor (2011) and Naylor *et al.* (2016) employed marine paint as a tracer to document evidence of periodic detachment, entrainment, deposition and the breakdown of boulders. The latter study quantified the transport distance of fine and medium-sized boulders and is thought to be the first intra-storm assessment of boulder transport. Using painted tracers an 81% recovery rate (n=39/48) was achieved over a 4 day monitoring period. Despite the valuable insights gained from these studies the paint methodology has limitations, as follows: (1) the reliance on visual detection prevents relocation of buried tracers resulting in reduced rates of recovery; (2) the paint coating may arouse unwanted attention and encourage anthropogenic transport; (3) prolonged exposure leads to paint abrasion limiting the longevity of the study; (4) being visually obtrusive, issues may arise with gaining authorisation for the use of painted tracers in sensitive and designated coastal locations. These factors suggest an alternative, more discreet technique is required for effectively tracing boulder displacement over monthly and annual timescales, RFID tagging provides a viable alternative. Furthermore, with a non-visual mode of detection, RFID tags allow for the relocation of buried clasts, resulting in improved rates of recovery (Bray *et al.,* 1996).

Despite the potential of RFID tags for quantifying boulder transport (Paris *et al.,* 2011) their use has focused predominantly on mixed gravels and cobbles (Allan *et al.,* 2006; Miller *et al.,* 2011; Dolphin *et al.,* 2016) rather than boulder-sized clasts (Table I). The limited use of RFIDs to monitor boulder displacement may be due to perceived limitations with the technique, identified by Paris *et al.* (2011) and Naylor *et al.* (2016). Specifically, the ability of the tags to remain operational, concerns with clast breakdown and the ability to recover tagged material in a short tidal window. To date, we are aware of only one study that has incorporated the use of RFIDs in monitoring clast mobility that extends into the boulder size range (Brayne, 2015); where the maximum size classification used was fine boulders with an intermediate axis up to 0.51 m. We broaden the scope of this previous work and allay concerns with the use of RFIDs having conducted the first known field investigation applying RFID tagging to boulder-sized clasts only, from fine through to very coarse boulders.

We embedded RFID tags in 104 limestone boulders across two sites, Bembridge Ledge (n=50) and Black Rock (n=54) at Bembridge, Isle of Wight, UK. Boulders were selected from the indigenous sediment to reflect a range of shapes, particle sizes and morphological settings. Between July 2015 and May 2017 fifteen topographic surveys were conducted to relocate tagged boulders. Recovered boulder positions were recorded using DGNSS; the collated data providing a spatial and temporal context to boulder displacement. This coordinate data was processed using a tailored python script (the script is included in the Supplementary documentation, Data S1) which calculates the distance and azimuth between successive points.

The focus of this paper is the RFID methodology. We describe in detail the procedures undertaken and recommend a series of considerations, highlighting best practice for successful field tag deployment and monitoring. We draw upon incidents of mobility from the field surveys to illustrate the capability and effectiveness of the methodology for use in future boulder transport studies.

RFID Methodology

RFID operational overview

The term RFID describes the various technologies that utilise radio waves to identify objects (Aluf, 2017). It has been integrated into numerous mainstream applications, primarily as a means of asset tracking. RFID technology comprises four key components, a transponder, more commonly referred to as a tag, an antenna, a reader and a user interface (PDA), Figure 1.

1 RFID TAGS (transponder): the tags enclosed circuitry is housed within a hermetically sealed glass casing. Each tag is pre-programmed with a unique 16-digit ID code allowing for the unequivocal identification of an individual object, in this instance a boulder.
2 POLE ANTENNA: connected to the reader via a cable the circuitry housed within the antenna tubing emits and receives electromagnetic signals via the circular loop. The pole is operated in the field in a sweeping movement, similar to that of a conventional metal detector.
3 BACKPACK READER: powered by a 14.8 volt lithium polymer (Li-Po) battery the reader is housed in a backpack. It produces a low frequency (134.2 kHz) electromagnetic signal which is transmitted via the pole antenna.
4 HANDHELD COMPUTER (PDA): featuring specialist software that enables the identification of the unique tag ID number. This is wirelessly connected to the reader via a Bluetooth adapter.

Tag detection occurs when the pole antenna comes within range of a deployed tag, detection range details are documented in Table II. The emitted electromagnetic signal from

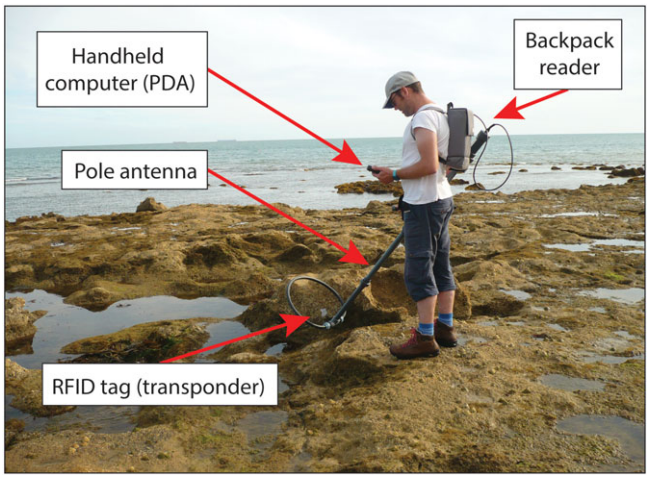

Figure 1. RFID detection equipment. (Photo, M. Schaefer). [Colour figure can be viewed at wileyonlinelibrary.com]

Table II. The effect of tag approach direction on detection range; all values expressed in metres

	Mean detection range (m)								
Tag approach	Tag 1	Tag 2	Tag 3	Tag 4	Tag 5	Mean	Min. range	Max. range	Std deviation
North	0.78	0.78	0.78	0.78	0.76	0.77	0.72	0.84	0.03
East	0.42	0.44	0.43	0.43	0.42	0.43	0.36	0.5	0.03
South	0.61	0.62	0.62	0.63	0.62	0.62	0.56	0.69	0.03
West	0.35	0.34	0.35	0.34	0.34	0.34	0.29	0.41	0.03

the loop of the pole antenna provides sufficient power to prompt tag activation. The tag becomes energised and transmits a return signal containing the unique tag ID code which is received by the antenna and relayed to the reader. An audible alarm also alerts the user to the detection of a tag. The return signal is translated by the reader and transmitted via the Bluetooth functionality to the PDA or alternative mobile device, notifying the user of the tag ID code (Figure 2).

RFID tags can be described as active or passive in their operation (Nichols, 2004). Active tags require a power source (e.g. a battery) which renders them impractical for sediment tracking purposes based on size, cost and longevity of operation. Passive tags, also referred to as Passive Integrated Transponder (PIT) tags have no internal power source making them smaller (tag sizes of 12 mm, 23 mm and 32 mm in length are available). Without the need for a battery the tags have a potentially unlimited operational capacity (Want, 2006) although Allan *et al.* (2006) suggest a more conservative 50 year lifespan.

RFID systems are available from a variety of sources. We selected a field ready solution supplied by Oregon RFID as the manufacturer's specification fulfilled our criteria of tag detection ranges approaching 1 m.

Typically, existing tracer techniques rely on the collection and removal of sediment from a study site for tagging in the comfort of a laboratory with access to a range of specialist equipment (Allan *et al.,* 2006; Dickson *et al.,* 2011). Size constraints dictate boulder tagging must be conducted in the field. This generates a number of novel issues which require consideration prior to, and during tag deployment to ensure a successful monitoring campaign. These will be addressed herein.

Site selection and description

A pre-requisite of any proposed site is the presence of coarse clastic material known to be mobile during periods of increased wave activity. Accessibility is a key consideration as site visits may be required at short notice in response to storm activity. Further consideration is afforded to the locality of wave recording devices to establish hydrodynamic conditions relating to specific storm events which provides insight to the wave thresholds required to initiate transport.

Bembridge is located at the most easterly point of the Isle of Wight (50.6883°N, -1.06982°W), Figure 3. It was selected as it fulfils the aforementioned criteria. We selected two field sites, Bembridge Ledge and Black Rock Ledge upon which 104 RFID tags were inserted into boulders of varying size and shape (n=50 and n=54, respectively). Each site covers an area of approximately 0.1 km^2. Boulders are distributed across both sites either as individual, solitary clasts, or collectively as clusters or as distinct assemblages such as boulder ridges. The nearest wave buoy, operated by the Channel Coast Observatory (CCO) is located approximately 5 km to the southwest of the study site at Sandown Bay. The buoy is positioned 1.2 km from the coast in a water depth of 10.7 m (chart datum). There is also a tidal gauge recording wave and tidal parameters located on Sandown Pier (Figure 3(c)). Wave, tidal and selected meteorological parameters are recorded every 30 min (CCO, 2017a).

The area is classified as meso-tidal with a spring and neap tidal range of 3.7 m and 1.8 m, respectively. Current research relating to boulder transport has focused on site locations with considerable fetches (Noormets *et al.,* 2004; Scheffers *et al.,* 2009; Switzer and Burston, 2010). Comparably, Bembridge has a limited fetch (Figure 3(d)), its eastern aspect providing shelter from large Atlantic swell waves and the prevailing southwesterly wind and wave direction. Bembridge Ledge is east facing while Black Rock has a southern aspect which is more exposed to wave activity.

Average wave direction is dominant in the southern quadrant with a mean of 164° over the 22 month study period (July 2015–May 2017). Average significant wave height (H_s) was 0.6 m and a maximum wave height (H_{max}) of 6.8 m was recorded over the same period (CCO, 2017b).

A key feature of the Bembridge coastline is an extensive series of intertidal terraced shore platforms that extend up to 500 m seaward at its widest point. The platforms are

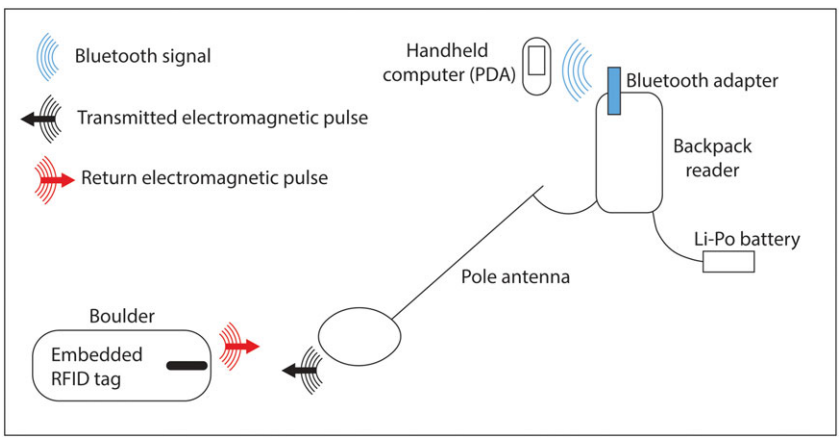

Figure 2. Schematic diagram of RFID operation illustrating signal transmittance to/from a boulder embedded RFID tag. [Colour figure can be viewed at wileyonlinelibrary.com]

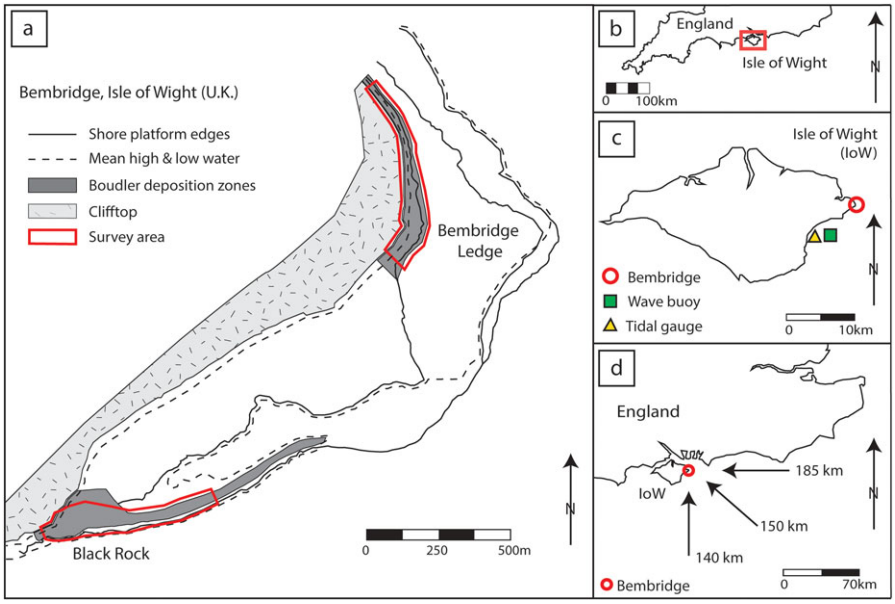

Figure 3. Bembridge study sites. (a) Black Rock and Bembridge Ledge – tagged boulders are located within the survey areas; (b) Isle of Wight's geographic location within the UK; (c) proximity of wave and tidal recording locations relative to the study site; (d) fetch distances to the study site. [Colour figure can be viewed at wileyonlinelibrary.com]

characterised by an abrupt terminus, akin to the type-B shore platform as described by Sunamura (1992). The platforms are formed of well jointed, near horizontally bedded Late Eocene Bembridge Limestone (Daley and Edwards, 1990; Armenteros and Daley, 1998). The limestone beds are interspersed by thin layers of Bembridge Marl which are preferentially eroded creating an overburden of the more consolidated limestone. The overburden, coupled with dense bedding and jointing facilitates the liberation of blocks from the shore platform edge (Trenhaile, 2002; Knight *et al.,* 2009; Hall, 2011). Block removal, or quarrying, occurs when waves break against fractured rock structures resulting in increased pressure within air-filled joints (Stephenson and Kirk, 2000; Knight and Burningham, 2011). Increased wave impact pressures promote crack propagation leading to boulder quarrying (Müller *et al.,* 2003). Many of the Bembridge boulders (including RFID tagged clasts) originate from the quarrying process, and are therefore, created, and subsequently transported and deposited by wave activity within the intertidal zone (Figure 4).

Tag selection

RFID tags used in sediment tracing are available in three sizes, 12 mm, 22 mm and 32 mm. The choice of tag size depends on (1) the size of clast to be tagged: the tag required needs to be smaller than the clast into which it is being inserted; (2) the likelihood of clast burial: the smaller the clast size the greater the likelihood of burial, therefore the vertical tag detection range requires consideration; (3) the required tag detection range: the distance across which a tag can be detected is contingent on a number of factors including tag size, tag orientation,

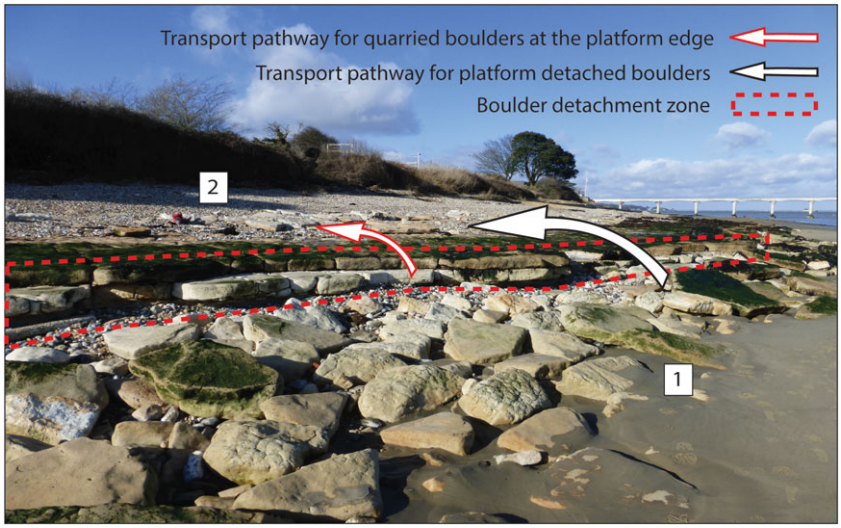

Figure 4. Boulder detachment, transport and deposition at Bembridge Ledge. The clearly defined bedding and jointing at the platform terminus facilitates the production of boulders via quarrying and undermining. (1) Detached boulders deposited seaward of the platform edge awaiting transport; (2) transported boulders deposited upon the gravel beach. Boulder transport pathways are highlighted. [Colour figure can be viewed at wileyonlinelibrary.com]

proximity of noise (e.g. electrical appliances), reader battery level and antenna diameter (Allan *et al.,* 2006; Chapuis *et al.,* 2014; Oregon RFID, 2017). To maximise the tag detection range we selected 32 mm tags thus increasing the likelihood of tag recovery (Chapuis *et al.,* 2014; Oregon RFID, 2017).

As part of the pre-deployment testing we conducted a series of laboratory trials to establish the significance of tag orientation on the detection range. We placed the 32 mm RFID tag horizontally on the floor aligned along the north–south axis with the visible copper wire circuitry (Figure 5) orientated north, 0°, replicating Chapuis *et al.* (2014). We approached the tag from the north, east, south and west with the antenna elevated 0.1–0.2 m above the ground. When the audible detection alarm was activated we recorded the distance from the end of loop antenna to the tag. Testing was conducted on five different tags with 20 approaches from the aforementioned cardinal directions. The results identified that approaching the tag 'head on' from the north towards the copper coil tag end provided a greater read range than from any other direction (Table II). We recorded a mean detection range of 0.77 m, within 15% of the manufacturer's published detection range of 0.89 m (Oregon RFID, 2017). Similar experimental analysis by Chapuis *et al.* (2014) suggested approaching the tag from the northeast maximises tag detection although this was based on 23 mm tags as opposed to 32 mm.

Before insertion within the boulder, tags were checked in the laboratory to ensure operational functionality by placing them within range of the antenna. The last four digits of the transmitted tag ID were noted. Tags were placed in a protective silicone sleeve to provide additional protection from impact forces during displacement.

The ends of the sleeved tag were capped with a waterproof sealant and allowed to cure. This created a waterproof seal around the tag providing further protection and prolonging operational use. The silicon sleeve was numbered with the last 4 digits of the tag ID code and the copper coiled end was marked for identification in the field at the time of insertion (Figure 5).

Boulder selection

Before selecting boulders for tagging a number of factors should be considered as they can affect the ability to successfully relocate and record boulders within a single tidal cycle. These include site terrain, tidal regime, spatial distribution of tagged boulders, the number of RFID tag detectors, and the availability of field assistance. In addition, wave climate requires consideration as this has the ability to disperse tracers across a wider area extending the time required to relocate tagged clasts.

A key factor in tracer studies relates to the effectiveness of the introduced material to accurately reflect the physical properties, namely size and shape of the indigenous sediment (Black *et al.,* 2007). This was achieved by measuring a random selection of 100 indigenous boulders at each of the two Bembridge sites, recording the long (*L*), intermediate (*I*) and short (*S*) axial dimensions. These measurements were also used to establish boulder shape as characterised by Zingg (1935). Comparisons of size and shape between the indigenous and tagged boulders are presented in Table III. The values express a degree of similarity between the two populations.

Samples of the Bembridge Limestone were analysed in the laboratory to determine rock density using the displacement method. Repeated experimentation produced values of 2.4 g/cm^3. All tagged boulders were formed of the local Bembridge Limestone.

The number of boulders selected for tagging was based on the ability to recover the entire array within a single tidal

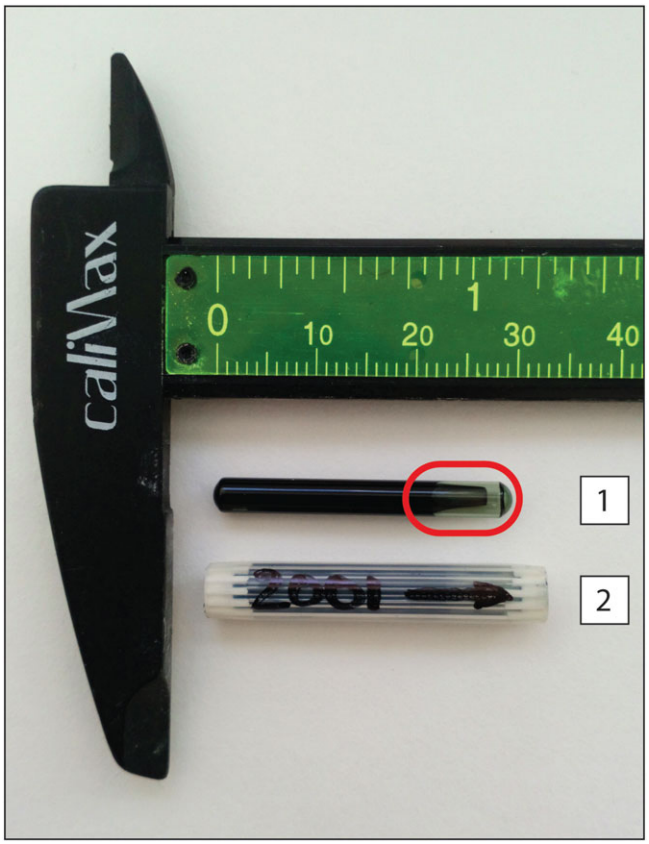

Figure 5. RFID tag; (1) 32 mm RFID tag, the copper coils are located in the transparent end of the tag, circled; (2) RFID tag within a numbered protective silicone sleeve. [Colour figure can be viewed at wileyonlinelibrary.com]

Table III. Particle size and shape of indigenous and tagged boulders, mean boulder size classifications are based on the length of the intermediate axis

		Bembridge Ledge	Black Rock
Size	Mean indigenous boulder size (m)	0.76	0.84
	Mean tagged boulder size (m)	0.78	0.82
Shape (Zingg, 1935)	Disc (% indigenous/tagged)	(65/66)	(49/46)
	Blade (% indigenous/tagged)	(32/30)	(19/15)
	Rod (% indigenous/tagged)	(1/2)	(13/11)
	Sphere (% indigenous/tagged)	(2/2)	(19/28)

window. With time allocated to setting up the survey equipment and based on a working team of two persons we estimated it would be possible to relocate between 50 and 55 boulders. Further consideration should be reserved for tagging boulders in close proximity to one another. This relates to the detection range of the RFID tags. For example, given an approximate tag detection range of 0.75 m, upon detection, any two or more tagged boulders within that range may simultaneous transmit a tag ID code. These multiple transmissions create a shadowing effect whereby both tags are activated yet only one code can be received and displayed on the PDA (Lamarre *et al.,* 2005; Chapuis *et al.,* 2014; Dolphin *et al.,* 2016). Therefore, it is suggested the minimum distance between tagged boulders should exceed the mean detection range of the deployed tags.

In selecting boulders for tagging we aimed to represent a range of zones from both sites as Naylor *et al*. (2016) identify the significance of morphological setting in controlling boulder mobility. These locations also serve to establish a pre-transport setting for each tagged boulder. The significance of the pre-transport setting is well documented when used in conjunction with hydrodynamic equations to calculate the magnitude of retrospective wave conditions responsible for boulder transport (Nott, 2003a; Switzer and Burston, 2010; Spiske and Bahlburg, 2011; Nandasena *et al.,* 2011b). The boulder zones are summarised in Table IV.

Owing to differences in local conditions it was not possible to maintain consistency of selected boulders between sites, therefore some classifications are underrepresented. This is due to the limited availability and accessibility of suitable boulders to tag, e.g. the lower platform elevation at Black Rock restricts access to boulders located seaward of the shore platform to only the lowest spring tides.

Finally, boulder selection was limited to those boulders that were deemed too large to be moved by human intervention. All tagged boulders had an intermediate axis >0.25 m, this restricted the agent of transport to wave activity alone.

Field tag deployment

The current literature refers to the deployment of RFID tags in gravel and cobbles only. There are no published accounts relating to the specific requirements for boulder tagging. We aim to address this with a detailed review of the tagging procedure demonstrating some key refinements that are required for boulder sized sediments.

Table IV. RFID tagged morphological boulder zones, pre-transport setting and description; Bembridge Ledge (BL) and Black Rock (BR)

Morphological boulder zones	Pre-transport setting	Description	Number (BL/BR)	Figure
Located on the seaward side of the shore platform.	Platform edge (detached)	Boulders located at the edge of the shore platform which are fully detached and awaiting transport. The tagged clasts located here are impeded in their transport potential by the raised shore platform edge.	13/3	4 (1)
Located at the shore platform edge.	Platform edge (joint bound)	Described by Nott (2003a) as joint bound blocks. The geologically discontinuous lithology at Bembridge creates angular blocks at the platform edge. These blocks may, or may not, be fully detached from the platform edge being constrained on one or more sides by the surrounding strata.	4/2	6 and 9 (inset)
Located on the shore platform (limited transport potential owing to local topography and/or morphology).	Platform top (constrained)	Boulders deposited on the platform, the transport of which is considered to be restricted by local topography and/or morphological features, i.e. positioned in a depression or imbricate against a rock feature (scarp) or other boulder/s (Trenhaile, 2016).	18/25	11a
Located on the shore platform (greater transport potential owing to local topography and/or morphology).	Platform top (unconstrained)	Boulders deposited on the platform, further transport is unhindered by local topography and/or morphological features (Trenhaile, 2016).	15/24	7

First, holes have to be drilled into boulders in the field to enable tag insertion. In preparation, drill tests were conducted within the laboratory on samples of the indigenous boulder rock type (Bembridge Limestone). These tests provided a valuable assessment on the operational capacity of the drill and the longevity of the battery and drill bits. Testing identified the necessity for a quality, industrial cordless drill and drill bits. We found the Makita 8391DWPQ 18v Ni-Cad Cordless Hammer Drill and DeWalt Extreme II 7 mm drill bits performed particularly well.

Due to the number of boulders to be tagged in the field and based on the preceding laboratory tests a number of spare drill bits and a second drill battery were required together with a means of recharging drill batteries in the field. We achieved this using a 12 V car battery connected to a power inverter which converts DC power to AC enabling continued recharging of the spare drill battery while the other is in use. The additional weight may prompt logistical considerations particularly where a study site has restricted access and/or limited field assistance is available. Due to the changeable nature of weather conditions at coastal locations we kept the recharging equipment dry by securing it in a watertight receptacle.

The chosen location for tag insertion within the boulder is of great importance. To accurately quantify boulder transport it is necessary to relocate and record the same position on tagged boulders during each survey; we selected the tag insertion point (TIP) for this purpose. Tag insertion in the *L/I* plane should be avoided as in the event of transport the boulder may be overturned on to the *L/I* plane obstructing access to the TIP. To increase the likelihood of accessing the TIP the tag should be inserted in the *S*-axis parallel with the orientation of the *L*-axis (Figure 6). Knowing the location of tag insertion makes identifying the TIP easier should the boulder become colonised with algae and/or barnacles.

Once a suitable TIP was identified a drill hole was made to the required depth with a 7 mm drill bit (hole depth and width required is dependent on tag size). Excess dust was expelled from the hole prior to tag insertion to create a dust-free surface. A waterproof, silicon-based sealant (Evo-Stik Wet grab) was injected into the hole, filling to approximately 75%. The pre-prepared sleeved tag was inserted with the copper coils orientated towards the drilled exit hole. This was based on the increased read range of the tags positioned in this manner, as identified in Table II. Once embedded any excess sealant was removed. A further protective seal was applied using Plastic Padding Marine Epoxy creating an additional barrier to prevent the ingress of seawater (R. Brayne, 8 April 2014, pers. comm.). Before application the epoxy should be mixed as per the manufacturer's instruction. Curing time varies between products and depending on ambient temperature meaning incoming tides may not allow for the necessary curing times. Hence, it is important to use an epoxy resin that can, if necessary, be applied and cured underwater. Once embedded it is advisable to ensure the tag is detectable and the unique ID code can be transmitted from within the boulder prior to moving on to the next tag insertion. We suggest undertaking laboratory trials of the adhesive and protective properties of the chosen sealant and epoxy prior to full-scale field deployment.

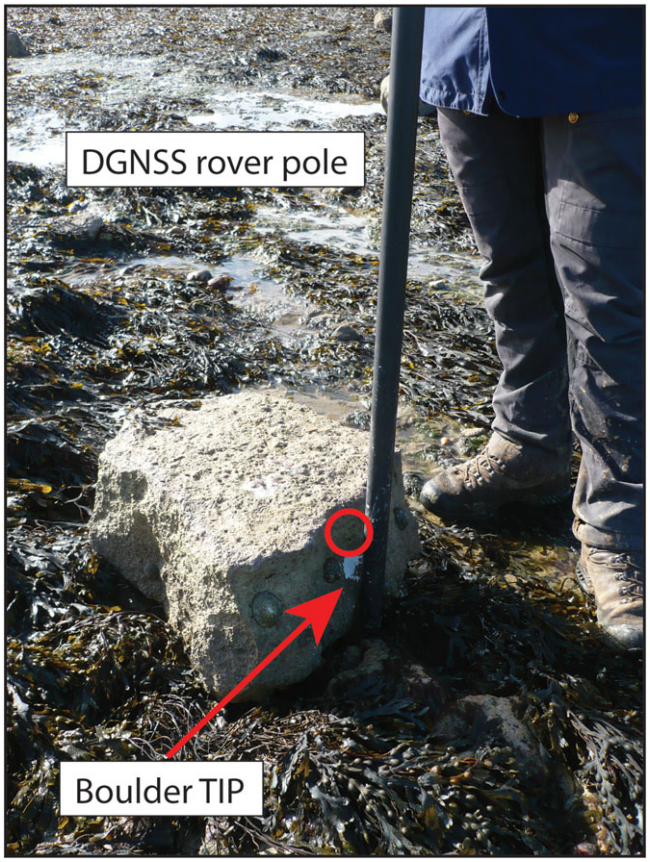

Figure 7. Recording the boulder location, the DGNSS pole is positioned against the TIP. The orientation hole is located above the TIP (circled), indicating the boulders upward orientation at the time of relocation. [Colour figure can be viewed at wileyonlinelibrary.com]

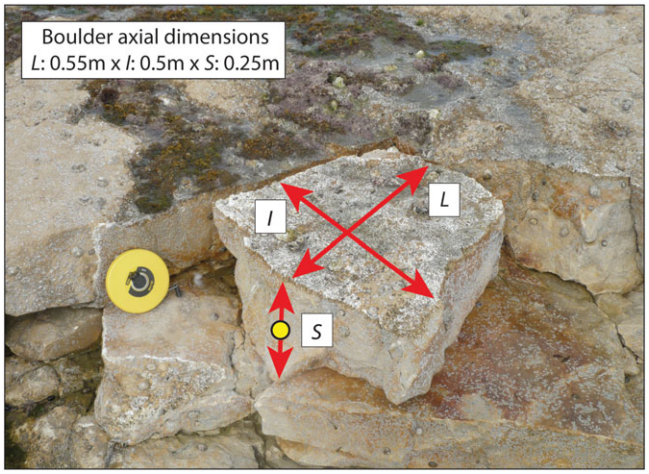

Figure 6. Recommended tag insertion point (TIP) within the S-axis indicated by the circle with the recorded boulder axial dimensions. [Colour figure can be viewed at wileyonlinelibrary.com]

Existing research has indicated that wave activity is capable of flipping, or overturning a range of boulder sizes (Sousa, 1979; Noormets *et al.,* 2004; Imamura *et al.,* 2008). Such events can be inferred by algal growth on a boulder's underside (Knight *et al.,* 2009), by the presence of biotic indicators (Mastronuzzi and Sansò, 2004) or using comparative photographic evidence (Cox *et al.,* 2018). The ability to identify overturning during entrainment provides a useful insight to the mode of transport. To establish when incidents of overturning occur we suggest drilling a secondary orientation hole, approximately 0.01 m deep above the TIP. This identifies the upward orientation of the boulder at the time of tag deployment. Any relocated boulder found with the orientation hole below the TIP can unequivocally be identified as being overturned during transport.

Recording tagged boulder characteristics

On completion of the tagging procedure a series of boulder characteristics were noted, as described in Table V.

Under favourable conditions the tag insertion procedure and collation of characteristics took approximately 5–8 min per boulder.

Tag retrieval surveys

The frequency of the retrieval surveys was dictated by a number of factors including favourable tides, the occurrence of storm activity and availability of field assistance. As part of this study 15 surveys were undertaken between July 2015 and May 2017 (seven at Bembridge Ledge and eight at Black Rock). Accessibility to tagged boulders limited surveys to periods of low water only.

To date RFID studies relocate tagged sediment by systematically scanning the survey area with the pole antenna in the same manner as a standard metal detector (Nichols, 2004; Dolphin *et al.,* 2016). To ensure a more productive use of time in the field we utilised the 'stake-out survey' functionality of the Topcon DGNSS. This allowed us to upload boulder coordinate data as recorded on the preceding survey to the DGNSS handheld interface. By accessing the uploaded data

Table V. Details the suggested boulder characteristics that should be recorded at the time of tag insertion

Item	Noted characteristics	Description	Use	Figure
1	Boulder axial dimensions	The long (*L*), intermediate (*I*) and short (*S*) axis dimensions are measured.	To establish boulder shape and approximate mass.	6
2	Rock type	Noted to determine rock density by conducting laboratory testing on rock samples using the displacement method.	Values used to calculate boulder mass.	N/A
3	Long (L) axis orientation	Recording the boulder orientation offers insight to the transport direction as mobilised boulders often have the *L*-axis aligned perpendicular or parallel to the direction of travel (Nott, 2003b).	Subsequent measurement of the *L*-axis orientation during relocation surveys can help establish where small rotational movements (entrainment) may have occurred between surveys.	N/A
4	Distinguishing features	Distinctive boulder shape, impact scars, abrasion markings or biological indicators such as algal growth, evidence of boring and/or the presence of organisms (e.g. limpets, barnacles).	This may suggest the direction or mode of transport and provide insight to the pre-transport setting and direction and/or mode of transport.	7 and 9
5	Morphological context	Is the boulder topographically constrained in its ability to be transported, e.g. buried, imbricate against other clasts, located within a depression or against a raised scarp? Accumulated sediment may result in boulder burial during subsequent surveys restricting mobility.	Provides detail on the morphological setting which is known to influence boulder mobility (Naylor *et al.,* 2016).	8, 9 and 11a
6	Boulder photograph	Individual boulder images capture a broader visual account of the boulder setting.	Used to compile a boulder identification inventory for each survey. This proved useful for tag relocation and comparative purposes throughout the study.	1, 6, 7, 8, 9 and 11
7	Record the boulder location using the TIP	The DGNSS rover pole is placed next to the TIP and the coordinate recorded (Figure 7). The last 4-digits of the unique tag ID code are entered to the DGNSS interface for processing following survey completion.	Provides a spatial and temporal account of the boulder location.	7 and 8
8	Noting the position of the orientation hole	Noting the location of the orientation hole relative to the TIP (above the TIP at time of tag deployment). This is of relevance when conducting relocation surveys.	Identifies incidents of boulder overturning during transport if orientated differently to previous survey.	7

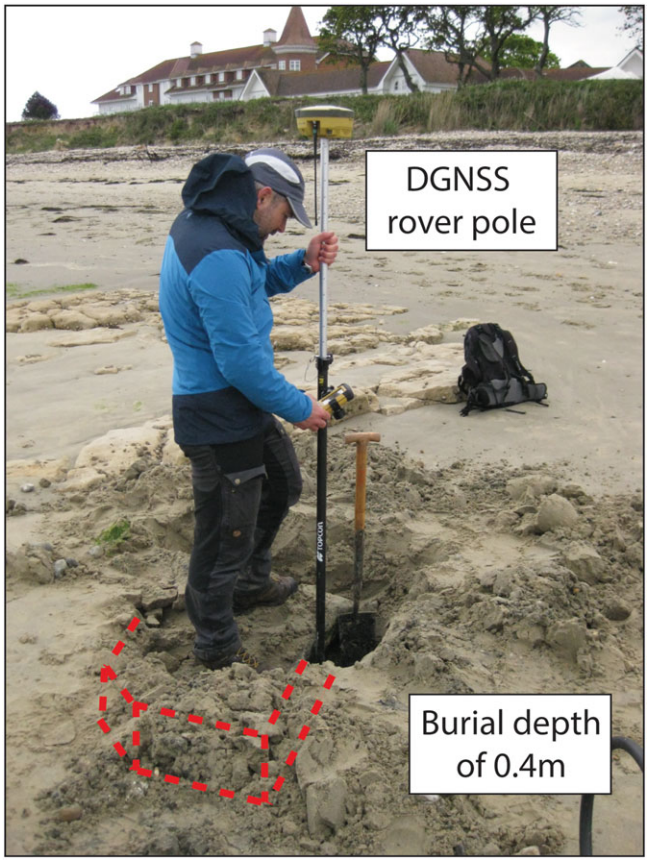

Figure 8. RFID tagged boulder relocated and excavated following the seasonal accretion of sand during the summer months. The TIP is being recorded with the DGNSS rover, the dashed line represents the remaining buried boulder. [Colour figure can be viewed at wileyonlinelibrary.com]

points in the field we were directed to the previously recorded coordinate of the selected boulder as indicated on the interface display screen. If the boulder was not relocated at that location the RFID detection equipment was used to scan the surrounding area until it was found. Once relocated, boulder characteristics 3–8 as described in Table V were documented.

At Bembridge Ledge we found that tagged boulders deposited towards the beach toe were subject to burial from the seasonal accretion of sediment. Despite being obscured from view we were able to relocate buried boulders using the RFID equipment to depths of up to 0.4 m. Upon relocation, the overlaying sediment was removed and the TIP recorded (Figure 8). Once the boulder location was recorded the excavated sediment was replaced.

Field survey equipment

In order to detect boulder movement in the centimetre range a DGNSS setup was required to provide a high survey resolution. Recreational GPS receivers or mobile phones with GNSS capabilities do not offer this level of precision (Schaefer and Woodyer, 2015). DGNSS uses static base stations with known positions to correct for the biases that cause GNSS errors (Kaplan and Hegarty, 2005; van Sickle, 2008). Boulder relocation surveys were conducted using a Topcon Hiper V in real-time kinematic (RTK) mode. This uses a local base station that sends out a correction signal in real time to a mobile GNSS receiver (rover), providing a relative horizontal accuracy of 5 mm, +/-0.5 ppm (Topcon, 2017).

Defining boulder transport

In coarse sediment transport studies the distinction between entrainment and transport is frequently unclear (Naylor *et al.*, 2016). By establishing a displacement threshold we are able to discriminate between the two, making it possible to establish when boulder transport has, or has not, occurred. Previous studies have monitored block displacement by embedding datalogging tri-axial accelerometers within clasts (Brayne, 2015; Stephenson and Abazović, 2016). The loggers record three-dimensional tilt and acceleration of the clast allowing the user to differentiate between incremental entrainment, such as motion about a fixed point, and major movement in a specific direction, akin to transport (Brayne, 2015).

Alternative methods have been employed that avoid the use of loggers, the cost of which can be prohibitive. Naylor *et al.* (2016) define transport whereby the distance moved and the combined root mean squared (RMSE) exceeds half the long axis length of a given clast, the RMSE being calculated from GPS, rover pole position and clast re-measurement error. This method was adopted as they were unable to re-record the same point on individual boulders. Unlike the aforementioned study we have a fixed point (the TIP) from which the boulder location can repeatedly be re-recorded. Therefore, in defining transport we combine the error from the relative accuracy of the DGNSS, the setup of the base station and the RMSE of re-surveying the TIP. The RMSE is based on recording four fixed points (two at each site) with the DGNSS as part of the field surveys; 30 measurements were recorded giving a RMSE of +/- 0.03 m in the horizontal and vertical axis, although maximum values of 0.08 m were recorded. Based on the cumulative error values we conservatively set the horizontal and vertical error at 0.1 m. This provides an entrainment/transport threshold

Table VI. Summary of boulder transport data from Bembridge Ledge and Black Rock from July 2015 to May 2017

BEMBRIDGE LEDGE (50 RFID tagged boulders)

Survey Period													
From	To	Boulders transported (% of total)	CTD (m): (Max IBTD*)	CTD (% of total)	Mean transport dist. (m)	Mean transport dist. Between surveys (m/day)	Mean mass of transported boulders (t): (Max. mass)	Mean direction of transport (°)	Overturning events	Max. Hs between survey period (m)[a]	Hmax between survey period (m)[b]	Date of storm activity (named where applicable).	Mean tag recovery rate
25th July '15	3rd Feb '16	21 (42)	49.2 (16.1)	42	2.3	0.25	0.5 (1.1)	229	6	3.3	5.4	3rd Jan '16	94%
3rd Feb '16	17th Feb '16	12 (24)	12.1 (7.5)	10	1.0	0.86	0.6 (1.2)	226	1	2.5	4.0	8th Feb' 16 (Imogen)	74%
17th Feb '16	1st Apr '16	13 (26)	6.3 (1.2)	5	0.5	0.14	0.6 (1.2)	177	0	4.2	6.6	28th Mar '16 (Katie)	78%
1st Apr '16	23rd Sept '16	11 (22)	5.5 (1.6)	5	0.5	0.03	0.5 (1.3)	192	0	1.8	3.0	10th Apr '16	68%
23rd Sept '16	25th Nov '16	13 (26)	12.7 (4.6)	11	1.0	0.20	0.5 (1.2)	233	3	4.0	6.8	20th Nov '16 (Angus)	90%
25th Nov '16	8th Feb '17	15 (30)	27.2 (8.9)	23	1.8	0.36	0.5 (1.2)	246	1	2.4	4.0	3rd Feb '17	100%
8th Feb '17	5th May '17	9 (18)	4.0 (2.3)	4	0.5	0.05	0.5 (1.3)	260	0	2.5	4.3	22nd Mar '17	100%
TOTAL		**94**	**117.0**		**1.1 (st. dev 0.7)**				**11**				**86%**

BLACK ROCK (54 RFID tagged boulders)

Survey Period													
From	To	Boulders transported (% of total)	CTD (m): (Max IBTD*)	CTD (% of total)	Mean transport dist. (m)	Mean transport dist. Between surveys (m/day)	Mean mass of transported boulders (t): (Max. mass)	Mean direction of transport (°)	Overturning events	Max. Hs between survey period (m)[a]	Hmax between survey period (m)[b]	Date of storm activity (named where applicable).	Mean tag recovery rate
10th July '15	3rd Dec '15	15 (28)	9.3 (2.9)	14	0.3	0.06	0.4 (1.8)	189	3	2.2	3.9	26th Jul '15	81%
3rd Dec '15	6th Jan '16	12 (22)	6.9 (2.8)	10	0.6	0.20	0.6 (1.8)	192	3	3.3	5.4	3rd Jan '16	93%
6th Jan '16	19th Feb '16	12 (22)	10.5 (4.0)	15	0.9	0.24	1.0 (5.0)	181	2	2.6	4.8	7th Jan '16	100%
19th Feb '16	31st May '16	12 (22)	27.7 (7.8)	41	2.3	0.27	2.0 (11.9)	240	2	4.2	6.6	28th Mar '16 (Katie)	100%
31st May '16	1st Sept '16	4 (7)	1.3 (0.8)	2	0.3	0.01	0.4 (0.7)	97	0	1.5	2.4	20th Aug '16	100%
1st Sept '16	9th Dec '16	6 (11)	9.6 (3.1)	14	1.6	0.10	3.4 (11.9)	194	1	4.0	6.8	20th Nov '16 (Angus)	98%
9th Dec '16	22nd Feb '17	7 (13)	1.2 (0.4)	2	0.2	0.02	0.7 (1.5)	143	0	2.4	4.0	3rd Feb '17	91%
22nd Feb '17	24th May '17	2 (4)	1.1 (0.8)	2	0.6	0.01	0.3 (0.4)	26	0	2.5	4.3	22nd Mar '17	100%
TOTAL		**70**	**67.6**		**0.9 (st. dev 0.7)**				**11**				**95%**
TOTALS		**164**	**184.6**		**1.0 (st. dev. 0.7)**				**22**				**91%**

[a]- Maximum significant wave height (m) – as recorded by the Channel Coast Observatory wave buoy (Sandown Bay).
[b]- Maximum wave height (m) – as recorded by the Channel Coast Observatory wave buoy (Sandown Bay).
*- NOTE: Additional detail on IBTD values is provided in the supplementary material.

whereby any movement calculated via the python script exceeding 0.1 m is defined as transported. Conversely, values below 0.1 m are deemed to be entrained and are not incorporated into any transport distance values.

The transport distance of the tagged boulders is calculated from the coordinate data from each survey which is input to the python script. The summed values for each boulder across all surveys we term the individual boulder transport distance (IBTD). The summed IBTD values for each survey we term the cumulative transport distance (CTD), Table VI.

Results

We report a range of metrics derived from the RFID boulder coordinate data obtained during successive field surveys. The data presented herein provides an insight to the feasibility of the methodology. In addition, we demonstrate the capability of the method by presenting examples of mobility that occurred during the field study which further augment the use of RFIDs in boulder transport monitoring. Table VI summarises cumulative boulder transport data and associated wave conditions. Supporting information (Tables A and B) details individual boulder specific transport data for all mobilised clasts.

Recovery rates

A total of 15 field surveys (Bembridge Ledge, 7 and Black Rock, 8) were conducted between July 2015 and May 2017 to relocate tagged boulders across the two study sites. We achieved a mean tag recovery rate of 91%, cumulatively recovering 714 of a possible 782 tagged boulders across all surveys at the two sites. Minimum/maximum tag recovery rates were 68%/100% at Bembridge Ledge, and 81%/100% at Black Rock (Table VI). Reduced tag recovery was attributed to the seasonal accretion of sediment leading to boulder burial at Bembridge Ledge and unfavourable and unsafe tidal conditions at Black Rock.

Boulder transport

Once relocated, RFID tag locations were recorded using DGNSS survey equipment. Successive surveys created a series of coordinates for each of the 104 tagged boulders. The python script automatically processed the recorded boulder coordinate data to produce a series of inter-survey transport statistics, including the IBTD (Table VI). We identified that 63% of the 104 tagged boulders were transported at least once (n=66/104), i.e. were mobile over distances exceeding 0.1 m. Over the study we recorded 164 individual transport events culminating in a total boulder transport distance of 184.6 m across the two sites.

At Bembridge Ledge 94 transport events were documented amounting to a total CTD of 117.0 m. Of that figure, the highest percentage of mobility (42%/49.3 m) occurred between July 2015 and 3 February 2016. Between these survey dates increased wave activity recorded by the CCO wave buoy occurred between 30 December 2015 and 7 January 2016. Peak storm activity occurred on 3 January 2016, when maximum significant wave heights (H_s) of 3.3 m and maximum wave height (H_{max}) of 5.4 m with a peak wave period of 7.7 s were recorded (CCO, 2017b). Surveys at Black Rock on 3 December 2015 and 6 January 2016 identify boulder transport amounting to 6.9 m during this period which coincides with the increased wave activity recorded on the 3 January 2016. Interestingly, peak storm waves occurred between low water and 2 h thereafter. The most significant transport distances were recorded in boulders located around low water on the exposed shore platform. This suggests boulder transport is influenced not only by storm wave activity but by tidal state at the time of peak storm intensity which determines where on the profile storm energy is focused. This corresponds with comparable work on the role of tidal state in beach morphodynamics (Kroon and Masselink, 2002; Castelle *et al.*, 2015; Masselink *et al.*, 2016b).

At Black Rock, 70 transport events were recorded during the study amounting to a total CTD of 67.6 m. Of that figure the highest percentage (41%/27.7 m) occurred between surveys conducted on 19 February and 31 May 2016 coinciding with increased wave energy associated with Storm Katie (28 March

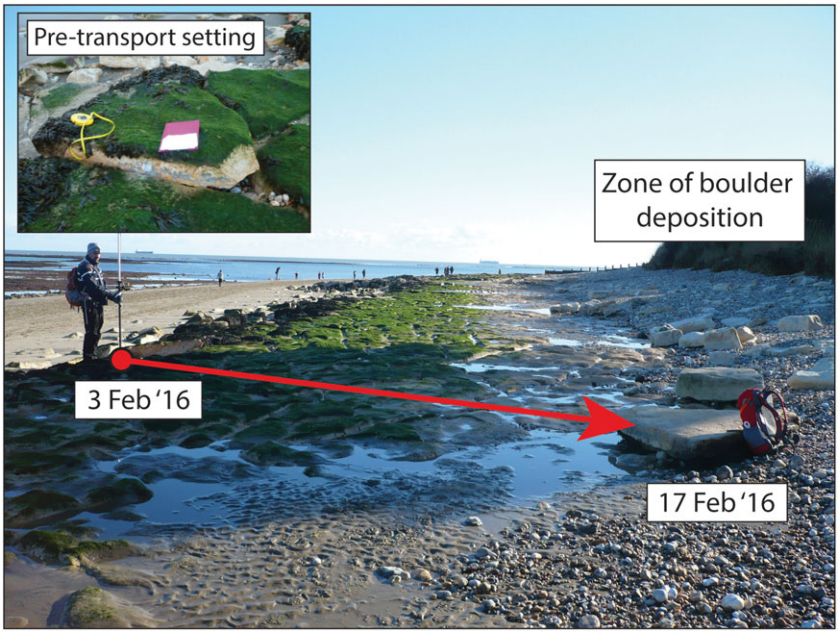

Figure 9. Evidence of transport at Bembridge Ledge (RFID tag ID: 1127). Boulder location recorded on 3 February 2016 (circle), relocated 7.2 m from its previously recorded position on 17 February 2016. The arrow indicates the direction of transport. Algal growth present on the underside of the boulder indicates overturning during transport. Inset: pre-transport setting, *in situ* boulder prior to displacement. Note the extensive algal growth on the exposed upper plane (pad for scale: 0.25 × 0.3 m). [Colour figure can be viewed at wileyonlinelibrary.com]

2016). For a period of 6.5 h H_s values exceeded 2.0 m, with a maximum H_s value of 4.2 m and H_{max} of 6.6 m being recorded; wave periods ranged between 6.3 and 10 s (CCO, 2017b). Conversely, surveys at Bembridge Ledge encompassing this period (17 February – 1 April 2016) identified 13 incidents of mobility covering a distance of 6.2 m, only 5% of the total CTD at the site. This disparity is thought to be the result of the southerly wind and wave direction during the storm event (mean: 170°). The southerly aspect of Black Rock being more exposed to the storm as opposed to the northeasterly orientation of Bembridge Ledge which was afforded a degree of protection.

Incidents of mobility – Bembridge Ledge

At Bembridge Ledge 76% (*n*=38/50) of the tagged boulders were mobile at least once. IBTD values ranged between 0.1 m and 21.5 m, mobile boulder mass ranged between an estimated 0.1 t and 1.3 t (Table VI).

Transport was documented in a boulder weighing approximately 1.2 t that had become detached from the platform edge yet remained *in situ* (Figure 9, inset). It was surveyed on 3 February 2016 however, the subsequent survey on 17 February 2016 identified transport of 7.2 m landward of its previous location (Figure 9). While mobile the boulder was overturned prior to deposition at the foot of the shingle beach where the slope angle increases. Overturning was identified by algal growth on the underside of the boulder and the orientation hole being located below the TIP, as opposed to above, as at the time of tag deployment. The transport event described coincided with increased wave activity associated with Storm Imogen (8 February 2016) when H_s of 2.5 m were recorded, with a wave period of 7 s. Further storm induced transport totalling 2.9 m was recorded for this clast amounting to an IBTD of 10.1 m over the 22 month monitoring period.

The coordinate data attributed to the aforementioned boulder was used to create a visual interpretation in ArcGIS which documents spatial and temporal boulder mobility. This was generated from the python script (Figure 10).

Incidents of mobility – Black Rock

At Black Rock 52% (*n*=28/54) of the tagged boulders were mobile at least once. IBTD values ranged between 0.1 m and 10.1 m. Mobile boulder mass ranged between an estimated 0.1 t and 11.9 t (Table VI).

A boulder located 20 m from the platform edge weighing an estimated 5 t was tagged at the commencement of the field campaign. Notably, the clast was not visible on the CCO aerial imagery captured in August 2013 and is thought to have been displaced and deposited during the winter storms of 2013–2014. The boulder location was recorded on 19 February 2016 identified by the circle in Figure 11(a). It was relocated on 31 May 2016 having been transported 6.4 m landward and overturned prior to deposition, imbricate against an extensive boulder ridge. The transport event described is thought to be attributed to Storm Katie (28 March 2016) when maximum H_s was recorded as 4.2 m, with a maximum wave period of 12.5 s. Further transport, post Storm Katie, was attributed to wave activity associated with Storm Angus on 20 November 2016, maximum H_s of 4.0 m and wave period of 6.8 s (CCO, 2017b) whereby the boulder was overturned 180° and deposited 2.5 m seawards from its previously recorded location, circle in Figure 11(b).

In both instances boulder transport was impeded by topographic (raised shingle beach at Bembridge Ledge) and morphological (boulder ridge at Black Rock) features. This emphasises the significance of localised morphology in restricting and controlling boulder transport potential affirming the findings of Pérez-Alberti and Trenhaile (2015b) and Naylor *et al*. (2016) who suggest such landforms exert a degree of control over boulder transport potential.

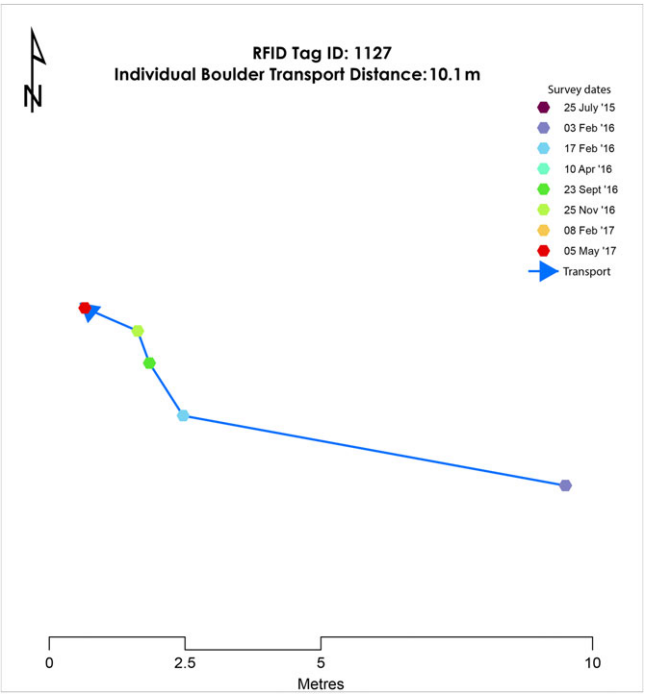

Figure 10. ArcGIS visual output documenting the direction of incremental step lengths and the Individual Boulder Transport Distance (IBTD) for the boulder pictured in Figure 9 (RFID tag ID: 1127). The absence of colour markers associated with specific survey dates indicates that no transport was recorded on that date. [Colour figure can be viewed at wileyonlinelibrary.com]

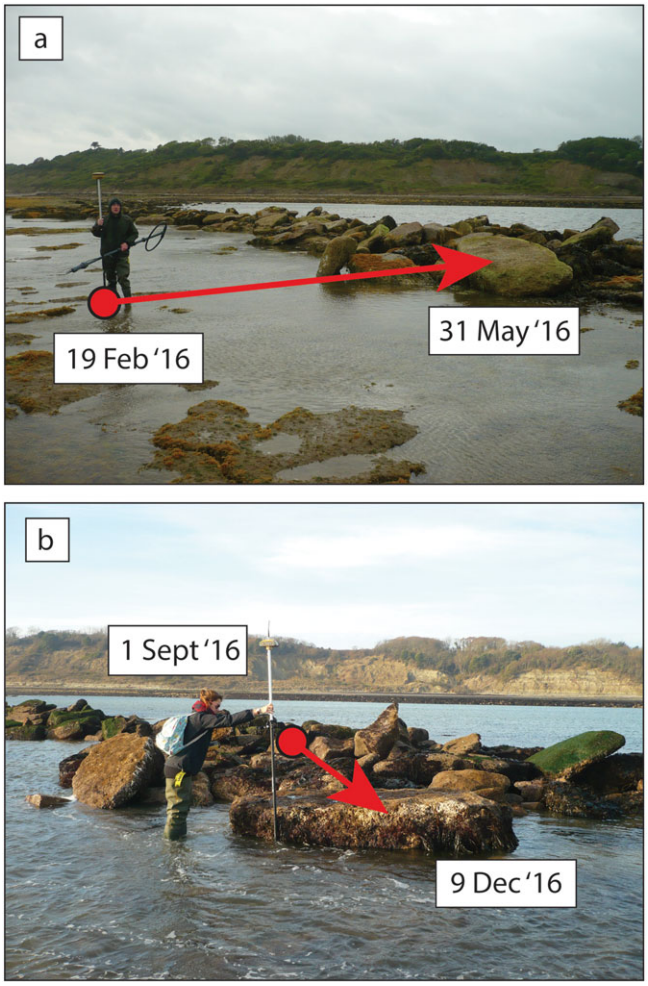

Figure 11. Evidence of transport at Black Rock (RFID tag ID: 1187). (a) Boulder location recorded on 19 February 2016 (circle), relocated 6.4 m from its previously recorded position on 31 May 2016. Further landward progression was hindered following deposition against a boulder ridge; (b) the same boulder recorded on 1 September 2016, (circle), relocated 2.5 m seaward from its previously recorded position on 9 December 2016. The arrows indicate the direction of transport. [Colour figure can be viewed at wileyonlinelibrary.com]

Discussion

Our proposed methodology, employing RFID tags embedded in an array of boulder-sized clasts has enabled us to identify and accurately quantify boulder mobility as a result of contemporary storm activity. Upon completion of the study we achieved a mean tracer recovery rate of 86% at Bembridge Ledge and 95% at Black Rock. Field data identified periodic boulder mobility resulting from contemporary storm activity despite the locations relatively low to moderate wave exposure in comparison with previously studied boulder transport sites.

Boulder transport

By establishing an entrainment/transport threshold we can reliably identify transport events and differentiate them from entrainment. Using the TIP we are able to relocate and record a specific point on each tagged boulder. This allows us to apply a universal displacement threshold that is applicable to each tagged boulder regardless of size. This is advantageous over alternative methods applied by Naylor *et al.* (2016) as it provides greater precision, particularly for coarser sized clasts, when defining the distance over which a boulder has been transported.

The calculated transport data for Bembridge Ledge exceeded that for Black Rock in terms of the number of transport events (94/70) and the distance over which those mobile boulders were displaced (117.0 m/67.6 m). This is, in part, due to the different lithologies of the two sites. The boulder-producing limestone outcrops differ in terms of the extent of jointing and bed thickness. Owing to the thinner, more discontinuous lithology at Bembridge Ledge smaller, tabular boulders are produced which have a lower transport threshold than the larger boulders produced at Black Rock, corroborating the significance of localised geology on boulder production (Stephenson and Naylor, 2011). In addition, obstructions including a greater number of detached clasts, irregular substrate and an extensive boulder ridge impede landward transport, particularly at Black Rock, resulting in a higher number of topographically constrained deposits (Trenhaile, 2016). The substrate varies between, and within sites. Bembridge Ledge is generally characterised by a smoother platform surface which promotes clast mobility. Comparatively, Black Rock has a larger area of pitted terrain which traps boulders impeding landward transport.

The close proximity of the recorded wave data to the study sites allows us to infer the probable agent of transport and identify the wave conditions under which boulder mobility occurred. Furthermore, by incorporating a boulder orientation indicator we were able to identify 22 incidents of boulders being overturned during transport, 11 at each site; 68% of these occurring between July 2015 and 19 February 2016. This

constitutes overturning in 13% of the recorded movements suggesting it is significant but relatively infrequent. Understanding how boulders respond to hydrodynamic conditions under which they have been transported is of considerable significance when applying numerical models to hindcast wave characteristics such as height and/or velocity (Goto *et al.,* 2009; Nandasena *et al.,* 2011a, 2011b).

Addressing limitations and uncertainties

Before commencement of the study we had reservations regarding the suitability of the RFID tagging technology to monitor boulder transport. Paris *et al.* (2011) and Naylor *et al.* (2016) describe a number of potential issues with the technique which we are now able to allay.

1 Would RFID tags withstand the harsh coastal conditions and remain operational throughout the study?

Despite the successful use of RFID tags in long-term coastal sediment monitoring (Allan *et al.,* 2006; Dolphin *et al.,* 2016), and our pre-deployment sealant checks, concerns remained regarding how the unfavourable conditions and prolonged exposure may affect tag operation and/or retention within the boulder. However, we experienced no issues with tag functionality during the survey period. With the exception of five lost tags, which we were able to replace, the remaining 99 tags remained fully operational and traceable throughout the study. Tag loss was attributed to poor sealant adhesion, perhaps as a result of insufficient curing times. We have since trialled a vinylester chemical anchor resin (ProVenture PRO V200) rather than the widely available silicone sealant. The resin has performed well in laboratory tests involving wetting and drying in saltwater solutions and has since been deployed in the field to replace the lost tags and to date has functioned well.

2 How effective would the RFID equipment be in relocating tagged boulders, particularly buried clasts?

The RFID equipment performed well in the field. Throughout the survey period it was apparent that concerns over relocating tagged boulders related to environmental factors beyond our control rather than limitations with the equipment and/or methodology. At Bembridge Ledge we frequently encountered incidents of burial following the accretion of sand and shingle. However, we were able to detect buried clasts up to a depth of 0.4 m. Owing to the extent of burial and time constraints it was not always possible to excavate the overlying sediment; additional manpower may have offered increased opportunity to excavate buried clasts. Black Rock recovery rates were reduced as a result of unfavourable tidal states due to the low elevation of an area of the field site in proximity to mean low water. On occasion this created hazardous surveying conditions rendering a number of boulders inaccessible. Greater consideration of tagged boulder location relative to mean low water may have reduced the likelihood of such an occurrence and improved rates of tag recovery.

3 Would clast breakdown impact on recovery rates?

We documented clast breakage in one of the 104 tagged boulders. The limited mobility of the clast (IBTD – 0.7 m) suggests breakdown was not attributed to impact during transport but due to the inherent weaknesses within the boulder; breakdown occurred along a number of structural joints.

There was no evidence to suggest drilling for tag insertion initiated boulder breakdown, as encountered by Cassel *et al.* (2017) as we took care to avoid drilling through any discontinuity planes. This suggests clasts exhibiting structural joints should be avoided when selecting boulders to tag.

4 Would it be possible to relocate and document the tagged boulders within a single tidal window?

The 'stake-out survey' functionality on the DGNSS hastened the boulder recovery process allowing us to maximise the time available in the field. It enabled us to recover tagged boulders within our 0.1 km^2 survey area with greater ease than adopting a random search approach. Had we not incorporated this feature into the methodology our ability to relocate tagged boulders would have been compromised.

The overall performance of RFID tagged boulders has been encouraging. Coupled with our proposed methodology they have provided new data on the extent to which boulders are transported in the intertidal zone by contemporary storm events. Additionally, they have provided insight to the mode of transport when displaced through the addition of an orientation indicator. The success of this deployment has enabled the study to continue into a third year. It is anticipated that with regular monitoring and maintenance of the tagged boulder array the study can continue indefinitely ensuring this will be the first known long-term study using RFID tagging to quantify boulder transport resulting from storm activity.

Conclusion

Drawing upon previous RFID transport studies and the findings presented here we assert that RFID technology and our methodology are an efficient and effective means of monitoring and quantifying the response of intertidal boulders to contemporary storm events. Using RFID tagged boulders we have been able to identify transport episodes resulting from periods of increased wave activity. The collated data has enabled the production of vector diagrams via a python script which detail the distance and direction of boulder transport.

The existing literature relating to boulder transport focuses on coastlines subjected to considerable storm induced wave energy (Etienne and Paris, 2010; Goto *et al.,* 2011; Knight and Burningham, 2011; Cox *et al.,* 2012). Significantly, the RFID methodology has enabled us to identify boulder detachment, transport and overturning at a relatively sheltered, fetch limited intertidal site subjected to moderate wave conditions. This demonstrates that contemporary storm events have a far greater ability to mobilise boulders than had previously been realised.

To further augment the methodology we recommend additional deployments in more exposed settings with larger boulders subjected to higher wave energy regimes. Furthermore, the methodology could be extended to use in the supratidal zone for the long-term monitoring of cliff-top boulder deposits such as those identified by Autret *et al.* (2018) and Cox *et al.* (2018). This would provide greater understanding on the impact, ability and associated risk of extreme wave events to mobilise boulders which may require a reassessment of our current understanding of storm wave hydrodynamics.

The methodology can also be utilised with emerging technologies, such as UAV monitoring (Pérez-Alberti and Trenhaile, 2015a, 2015b; Biolchi *et al.,* 2016) to provide greater spatial resolution on the mechanisms that facilitate the transport of intertidal boulders. Furthermore, deployment in coastal revetment blocks could help mitigate against damage or loss to coastal defence engineering works.

This study has highlighted the feasibility of both the RFID technology and our methodology to provide coastal researchers with a new field technique to accurately assess boulder mobility. By adopting the methodology the opportunity exists for researchers to clearly define and quantify boulder transport pathways and provide clarity on the impacts and responses of contemporary storm events in shaping rocky coastal landforms.

Footnote – Permissions

Under the Marine Licensing (Exempted Activities) Order, 2011 the deployment of scientific equipment, including sediment tracers such as RFIDs is deemed a Category 2 exemption and may not require a marine licence (Marine Licensing Order, 2011). However, owing to the sensitive nature of the study site we obtained an exemption from the Marine Management Organisation (MMO) and sought approval from Natural England prior to tag deployment.

Acknowledgements—The authors thank the British Society of Geomorphology and the Royal Geographical Society who assisted with funding the field work element of the study. The authors wish to extend their gratitude to those that provided invaluable field assistance, without their input the research would not have been possible; Tom Thorp, Liam Matear, Louise Richards, Elizabeth Inwards, Kathrine Bell, Lauren Knight, Paul Carter, Paul Weber and Alex Hilawi. We are also sincerely grateful to the anonymous reviewers for their insightful comments and suggestions which have greatly improved this paper.

References

Allan JC, Hart R, Tranquili JV. 2006. The use of Passive Integrated Transponder (PIT) tags to trace cobble transport in a mixed sand-and-gravel beach on the high-energy Oregon coast, USA. *Marine Geology* **232**: 63–86. https://doi.org/10.1016/j.margeo.2006.07.005.

Aluf O (ed). 2017. RFID antennas systems descriptions and analysis. In *Microwave RF Antennas and Circuits*. Springer International Publishing: 1–15. https://doi.org/10.1007/978-3-319-45427-6_1

Armenteros I, Daley B. 1998. Pedogenic modification and structure evolution in palustrine facies as exemplified by the Bembridge Limestone (Late Eocene) of the Isle of Wight, southern England. *Sedimentary Geology* **119**(3): 275–295. https://doi.org/10.1016/S0037-0738(98)00067-0.

Autret R, Dodet G, Fichaut B, Suanez S, David L, Leckler F, Ardhuin F, Ammann J, Grandjean P, Allemand P, Filipot JF. 2016. A comprehensive hydro-geomorphic study of cliff-top storm deposits on Banneg Island during winter 2013–2014. *Marine Geology* **382**: 37–55. https://doi.org/10.1016/j.margeo.2016.09.014.

Autret R, Dodet G, Suanez S, Roudaut G, Fichaut B. 2018. Long-term variability of supratidal coastal boulder activation in Brittany (France). *Geomorphology* **304**: 184–200. https://doi.org/10.1016/j.geomorph.2017.12.028.

Barbano MS, Pirrotta C, Gerardi F. 2010. Large boulders along the south-eastern Ionian coast of Sicily: storm or tsunami deposits? *Marine Geology* **275**(1): 140–154. https://doi.org/10.1016/j.margeo.2010.05.005.

Beniston M, Stephenson DB, Christensen OB, Ferro CA, Frei C, Goyette S, Halsnaes K, Holt T, Jylhä K, Koffi B, Palutikof J. 2007. Future extreme events in European climate: an exploration of regional climate model projections. *Climatic Change* **81**(1): 71–95. https://doi.org/10.1007/s10584-006-9226-z.

Biolchi S, Furlani S, Antonioli F, Baldassini N, Deguara JC, Devoto S, Di Stefano A, Evans J, Gambin T, Gauci R, Mastronuzzi G. 2016. Boulder accumulations related to extreme wave events on the eastern coast of Malta. *Natural Hazards and Earth System Sciences* **16**: 737–756.

Black KS, Athey S, Wilson P, Evans D. 2007. The use of particle tracking in sediment transport studies: a review. *Geological Society, London, Special Publications* **274**(1): 73–91. https://doi.org/10.1144/GSL.SP.2007.274.01.09.

Blair TC, McPherson JG. 1999. Grain-size and textural classification of coarse sedimentary particles. *Journal of Sedimentary Research* **69**(1): 6–19.

Bray MJ, Workman M, Smith J, Pope D. 1996. Field measurements of shingle transport using electronic tracers. In *Proceedings of the 31st MAFF Conference River and Coastal Engineers*, Vol. **1996**; 10–14.

Brayne RP. 2015. *The Relationship between Nearshore Wave Conditions and Coarse Clastic Beach Dynamics*. Unpublished PhD thesis, Exeter University.

Cassel M, Piégay H, Lavé J. 2017. Effects of transport and insertion of radio frequency identification (RFID) transponders on resistance and shape of natural and synthetic pebbles: applications for riverine and coastal bedload tracking. *Earth Surface Processes and Landforms* **42**(3): 399–413. https://doi.org/10.1002/esp.3989.

Castelle B, Marieu V, Bujan S, Splinter KD, Robinet A, Sénéchal N, Ferreira S. 2015. Impact of the winter 2013–2014 series of severe Western Europe storms on a double-barred sandy coast: beach and dune erosion and megacusp embayments. *Geomorphology* **238**: 135–148. https://doi.org/10.1016/j.geomorph.2015.03.006.

Channel Coast Observatory, CCO. 2017a. Regional Coastal Monitoring Programmes Sandown Bay. [Online]. Available at: https://www.channelcoast.org/data_management/real_time_data/charts/?chart=80&tab=info&disp_option= [Accessed: 20 May 2017].

Channel Coast Observatory, CCO. 2017b. Data management catalogue. [Online]. Available at: http://www.channelcoast.org/data_management/online_data_catalogue/metadata/search/index2.php [Accessed: 28 July 2017].

Chapuis M, Bright CJ, Hufnagel J, MacVicar B. 2014. Detection ranges and uncertainty of passive radio frequency identification (RFID) transponders for sediment tracking in gravel rivers and coastal environments. *Earth Surface Processes and Landforms* **39**(15): 2109–2120. https://doi.org/10.1002/esp.3620.

Ciavola P, Castiglione E. 2009. Sediment dynamics of mixed sand and gravel beaches at short time-scales. *Journal of Coastal Research*. Special Issue No. 56. Proceedings of the 10th International Coastal Symposium 2009 **II**: 1751–1755.

Cox R, Jahn KL, Watkins OG, Cox P. 2018. Extraordinary boulder transport by storm waves (West of Ireland, winter 2013–2014), and criteria for analysing coastal boulder deposits. *Earth-Science Reviews* **177**: 623–636. https://doi.org/10.1016/j.earscirev.2017.12.014.

Cox R, Zentner DB, Kirchner BJ, Cook MS. 2012. Boulder ridges on the Aran Islands (Ireland): recent movements caused by storm waves, not tsunamis. *The Journal of Geology* **120**(3): 249–272. https://doi.org/10.1086/664787.

Curtiss GM, Osborne PD, Horner-Devine AR. 2009. Seasonal patterns of coarse sediment transport on a mixed sand and gravel beach due to vessel wakes, wind waves, and tidal currents. *Marine Geology* **259**(1): 73–85. https://doi.org/10.1016/j.margeo.2008.12.009.

Daley B, Edwards N. 1990. The Bembridge Limestone (late eocene), Isle of Wight, southern England: a stratigraphical revision. *Tertiary Research* **12**(2): 51–64.

Dickson ME, Kench PS, Kantor MS. 2011. Longshore transport of cobbles on a mixed sand and gravel beach, southern Hawke Bay, New Zealand. *Marine Geology* **287**(1): 31–42. https://doi.org/10.1016/j.margeo.2011.06.009.

Dolphin T, Lee J, Phillips R, Taylor CJ, Dyer KR. 2016. Velocity of RFID tagged gravel in a non-uniform longshore transport system. *Journal of Coastal Research* **75**(sp1): 363–367. https://doi.org/10.2112/SI75-073.1.

Easterling DR, Meehl GA, Parmesan C, Changnon SA, Karl TR, Mearns LO. 2000. Climate extremes: observations, modeling, and impacts. *Science* **289**(5487): 2068–2074. https://doi.org/10.1126/science.289.5487.2068.

Engel M, May SM. 2012. Bonaire's boulder fields revisited: evidence for Holocene tsunami impact on the Leeward Antilles. *Quaternary Science Reviews* **54**: 126–141. https://doi.org/10.1016/j.quascirev.2011.12.011.

Etienne S, Buckley M, Paris R, Nandasena AK, Clark K, Strotz L, Chagué-Goff C, Goff J, Richmond B. 2011. The use of boulders for characterising past tsunamis: lessons from the 2004 Indian Ocean

and 2009 South Pacific tsunamis. *Earth-Science Reviews* **107**(1): 76–90. https://doi.org/10.1016/j.earscirev.2010.12.006.

Etienne S, Paris R. 2010. Boulder accumulations related to storms on the south coast of the Reykjanes Peninsula (Iceland). *Geomorphology* **114**(1): 55–70. https://doi.org/10.1016/j.geomorph.2009.02.008.

Fichaut B, Suanez S. 2011. Quarrying, transport and deposition of cliff-top storm deposits during extreme events: Banneg Island, Brittany. *Marine Geology* **283**(1): 36–55. https://doi.org/10.1016/j.margeo.2010.11.003.

Goto K, Miyagi K, Kawana T, Takahashi J, Imamura F. 2011. Emplacement and movement of boulders by known storm waves – field evidence from the Okinawa Islands, Japan. *Marine Geology* **283**(1): 66–78. https://doi.org/10.1016/j.margeo.2010.09.007.

Goto K, Okada K, Imamura F. 2009. Characteristics and hydrodynamics of boulders transported by storm waves at Kudaka Island, Japan. *Marine Geology* **262**(1): 14–24. https://doi.org/10.1016/j.margeo.2009.03.001.

Goto K, Sugawara D, Ikema S, Miyagi T. 2012. Sedimentary processes associated with sand and boulder deposits formed by the 2011 Tohoku-oki tsunami at Sabusawa Island, Japan. *Sedimentary Geology* **282**: 188–198. https://doi.org/10.1016/j.sedgeo.2012.03.017.

Hall AM. 2011. Storm wave currents, boulder movement and shore platform development: a case study from East Lothian, Scotland. *Marine Geology* **283**(1): 98–105. https://doi.org/10.1016/j.margeo.2010.10.024.

Han M, Yang DY, Yu J, Kim JW. 2017. Typhoon impact on a pure gravel beach as assessed through gravel movement and topographic change at Yeocha beach, South Coast of Korea. *Journal of Coastal Research* **33**(4): 889–906. https://doi.org/10.2112/JCOASTRES-D-16-00104.1.

Imamura F, Goto K, Ohkubo S. 2008. A numerical model for the transport of a boulder by tsunami. *Journal of Geophysical Research, Oceans* **113**(C1). https://doi.org/10.1029/2007JC004170.

Jolliffe IP. 1964. An experiment designed to compare the relative rates of movement of different sizes of beach pebble. *Proceedings of the Geologists' Association* **75**(1): 77–86. https://doi.org/10.1016/S0016-7878(64)80012-2.

Kaplan E, Hegarty C. 2005. *Understanding GPS: Principles and Applications*. Artech House: Boston, MA.

Kidson C, Carr AP, Smith DB. 1958. Further experiments using radioactive methods to detect the movement of shingle over the sea bed and alongshore. *The Geographical Journal* **124**(2): 210–218. https://doi.org/10.2307/1790248.

Knight J, Burningham H. 2011. Boulder dynamics on an Atlantic-facing rock coastline, northwest Ireland. *Marine Geology* **283**(1–4): 56–65.

Knight J, Burningham H, Barrett-Mold C. 2009. The geomorphology and controls on development of a boulder-strewn rock platform, NW Ireland. *Journal of Coastal Research* **1**: 1646–1650.

Kroon A, Masselink G. 2002. Morphodynamics of intertidal bar morphology on a macrotidal beach under low-energy wave conditions, North Lincolnshire, England. *Marine Geology* **190**(3–4): 591–608. https://doi.org/10.1016/S0025-3227(02)00475-9.

Lamarre H, MacVicar B, Roy AG. 2005. Using passive integrated transponder (PIT) tags to investigate sediment transport in gravel-bed rivers. *Journal of Sedimentary Research* **75**(4): 736–741. https://doi.org/10.2110/jsr.2005.059.

Lee MW, Bray M, Workman M, Collins MB, Pope D. 2000. Coastal shingle tracing: a case study using the 'Electronic Tracer System' (ETS). In *Tracers in Geomorphology*, Watson IDL (ed). Wiley: Chichester; 413–435.

Lee MW, Sear DA, Atkinson PM, Collins MB, Oakey RJ. 2007. Number of tracers required for the measurement of longshore transport distance on a shingle beach. *Marine Geology* **240**(1): 57–63. https://doi.org/10.1016/j.margeo.2007.02.010.

Liébault F, Bellot H, Chapuis M, Klotz S, Deschâtres M. 2012. Bedload tracing in a high-sediment-load mountain stream. *Earth Surface Processes and Landforms* **37**(4): 385–399. https://doi.org/10.1002/esp.2245.

Marine Licensing (Exempted Activities) Order 2011 (SI 2011/No. 409). Available at: http://www.legislation.gov.uk/uksi/2011/409/part/3/made [Accessed 2nd November, 2017].

Masselink G, Castelle B, Scott T, Dodet G, Suanez S, Jackson D, Floc'h F. 2016a. Extreme wave activity during 2013/2014 winter and morphological impacts along the Atlantic coast of Europe. *Geophysical Research Letters* **43**(5): 2135–2143. https://doi.org/10.1002/2015GL067492.

Masselink G, Scott T, Poate T, Russell P, Davidson M, Conley D. 2016b. The extreme 2013/2014 winter storms: hydrodynamic forcing and coastal response along the southwest coast of England. *Earth Surface Processes and Landforms* **41**(3): 378–391. https://doi.org/10.1002/esp.3836.

Mastronuzzi G, Sansò P. 2004. Large boulder accumulations by extreme waves along the Adriatic coast of southern Apulia (Italy). *Quaternary International* **120**(1): 173–184.

Miller IM, Warrick JA. 2012. Measuring sediment transport and bed disturbance with tracers on a mixed beach. *Marine Geology* **299**: 1–7. https://doi.org/10.1016/j.margeo.2012.01.002.

Miller IM, Warrick JA, Morgan C. 2011. Observations of coarse sediment movements on the mixed beach of the Elwha Delta, Washington. *Marine Geology* **282**(3): 201–214. https://doi.org/10.1016/j.margeo.2011.02.012.

Moses CA. 2014. The rock coast of the British Isles: shore platforms. *Geological Society, London, Memoirs* **40**(1): 39–56. https://doi.org/10.1144/M40.4.

Mottershead D, Bray M, Soar P, Farres PJ. 2014. Extreme wave events in the central Mediterranean: geomorphic evidence of tsunami on the Maltese Islands. *Zeitschrift für Geomorphologie* **58**(3): 385–411. https://doi.org/10.1127/0372-8854/2014/0129.

Müller G, Wolters G, Cooker MJ. 2003. Characteristics of pressure pulses propagating through water-filled cracks. *Coastal Engineering* **49**(1–2): 83–98. https://doi.org/10.1016/S0378-3839(03)00048-6.

Nandasena NA, Paris R, Tanaka N. 2011a. Numerical assessment of boulder transport by the 2004 Indian ocean tsunami in Lhok Nga, West Banda Aceh (Sumatra, Indonesia). *Computers and Geosciences* **37**(9): 1391–1399. https://doi.org/10.1016/j.cageo.2011.02.001.

Nandasena NA, Paris R, Tanaka N. 2011b. Reassessment of hydrodynamic equations: minimum flow velocity to initiate boulder transport by high energy events (storms, tsunamis). *Marine Geology* **281**(1): 70–84. https://doi.org/10.1016/j.margeo.2011.02.005.

Nandasena NA, Tanaka N, Sasaki Y, Osada M. 2013. Boulder transport by the 2011 Great East Japan tsunami: comprehensive field observations and whither model predictions? *Marine Geology* **346**: 292–309. https://doi.org/10.1016/j.margeo.2013.09.015.

Nathan Bradley D, Tucker GE. 2012. Measuring gravel transport and dispersion in a mountain river using passive radio tracers. *Earth Surface Processes and Landforms* **37**(10): 1034–1045. https://doi.org/10.1002/esp.3223.

Naylor LA, Stephenson WJ, Smith H, Way O, Mendelssohn J, Cowley A. 2016. Geomorphological control on boulder transport and coastal erosion before, during and after an extreme extra-tropical cyclone. *Earth Surface Processes and Landforms* **41**(5): 685–700. https://doi.org/10.1002/esp.3900.

Naylor LA, Stephenson WJ, Trenhaile AS. 2010. Rock coast geomorphology: recent advances and future research directions. *Geomorphology* **114**(1): 3–11. https://doi.org/10.1016/j.geomorph.2009.02.004.

Nichols MH. 2004. A radio frequency identification system for monitoring coarse sediment particle displacement. *Applied Engineering in Agriculture* **20**(6): 783–787. https://doi.org/10.13031/2013.17727.

Noormets R, Crook KA, Felton EA. 2004. Sedimentology of rocky shorelines: 3. Hydrodynamics of megaclast emplacement and transport on a shore platform, Oahu, Hawaii. *Sedimentary Geology* **172**(1–2): 41–65.

Nordstrom KF, Jackson NL. 1993. Distribution of surface pebbles with changes in wave energy on a sandy estuarine beach. *Journal of Sedimentary Research* **63**(6): 1152–1159.

Nott J. 2003a. Waves, coastal boulder deposits and the importance of the pre-transport setting. *Earth and Planetary Science Letters* **210**(1–2): 269–276. https://doi.org/10.1016/S0012-821X(03)00104-3.

Nott J. 2003b. Tsunami or storm waves? Determining the origin of a spectacular field of wave emplaced boulders using numerical storm surge and wave models and hydrodynamic transport equations. *Journal of Coastal Research* **19**: 348–356.

Oregon RFID. 2017. HDX Long Range Readers [Online]. Available at: https://www.oregonrfid.com/index.php?main_page=product_info&cPath=1&products_id=6&zenid=osn1jjl3mico7k8l9j0q5n3ho5 [Accessed: 12 September 2017].

Osborne PD. 2005. Transport of gravel and cobble on a mixed-sediment inner bank shoreline of a large inlet, Grays Harbor, Washington. *Marine Geology* **224**(1): 145–156. https://doi.org/10.1016/j.margeo.2005.08.004.

Paris R, Naylor LA, Stephenson WJ. 2011. Boulders as a signature of storms on rock coasts. *Marine Geology* **283**: 1–4): 1–11. https://doi.org/10.1016/j.margeo.2011.03.016.

Pérez-Alberti A, Trenhaile AS. 2015a. An initial evaluation of drone-based monitoring of boulder beaches in Galicia, north-western Spain. *Earth Surface Processes and Landforms* **40**(1): 105–111. https://doi.org/10.1002/esp.3654.

Pérez-Alberti A, Trenhaile AS. 2015b. Clast mobility within boulder beaches over two winters in Galicia, northwestern Spain. *Geomorphology* **248**: 411–426. https://doi.org/10.1016/j.geomorph.2015.08.001.

Russell RC. 1960. The use of fluorescent tracers for the measurement of littoral drift. *Coastal Engineering Proceedings* **1**(7): 24. https://doi.org/10.9753/icce.v7.24.

Schaefer M, Woodyer T. 2015. Assessing absolute and relative accuracy of recreation-grade and mobile phone GNSS devices: a method for informing device choice. *Area* **47**(2): 185–196. https://doi.org/10.1111/area.12172.

Scheffers A, Scheffers S, Kelletat D, Browne T. 2009. Wave-emplaced coarse debris and megaclasts in Ireland and Scotland: boulder transport in a high-energy littoral environment. *The Journal of Geology* **117**(5): 553–573. https://doi.org/10.1086/600865.

Sear DA, Lee MW, Oakley RJ, Carling PA, Collins MB. 2000. Coarse sediment tracing technology in littoral and fluvial environments: a review. In *Tracers in Geomorphology*, Watson IDL (ed). Wiley: Chichester; 21–55.

Shah-hosseini M, Morhange C, Beni AN, Marriner N, Lahijani H, Hamzeh M, Sabatier F. 2011. Coastal boulders as evidence for high-energy waves on the Iranian coast of Makran. *Marine Geology* **290**(1): 17–28. https://doi.org/10.1016/j.margeo.2011.10.003.

Sousa WP. 1979. Disturbance in marine intertidal boulder fields: the nonequilibrium maintenance of species diversity. *Ecology* **60**(6): 1225–1239. https://doi.org/10.2307/1936969.

Spiske M, Bahlburg H. 2011. A quasi-experimental setting of coarse clast transport by the 2010 Chile tsunami (Bucalemu, Central Chile). *Marine Geology* **289**(1–4): 72–85. https://doi.org/10.1016/j.margeo.2011.09.007.

Steers JA, Smith DB. 1956. Detection of movement of pebbles on the sea floor by radioactive methods. *The Geographical Journal* **122**(3): 343–345.

Stephenson WJ, Abazović A. 2016. Measuring coastal boulder movement under waves using tri-axial accelerometers. *Journal of Coastal Research* **75**(sp1): 607–611. https://doi.org/10.2112/SI75-122.1.

Stephenson WJ, Kirk RM. 2000. Development of shore platforms on Kaikoura Peninsula, South Island, New Zealand. *Part one: the role of waves. Geomorphology* **32**(1–2): 21–41. https://doi.org/10.1016/S0169-555X(99)00061-6.

Stephenson WJ, Naylor LA. 2011. Geological controls on boulder production in a rock coast setting: insights from South Wales, UK. *Marine Geology* **283**(1): 12–24. https://doi.org/10.1016/j.margeo.2010.07.001.

Sunamura T. 1992. *Geomorphology of Rocky Coasts*, Vol. **3**. John Wiley & Sons: Chichester.

Switzer AD, Burston JM. 2010. Competing mechanisms for boulder deposition on the southeast Australian coast. *Geomorphology* **114**(1–2): 42–54. https://doi.org/10.1016/j.geomorph.2009.02.009.

Topcon. 2017. HiPer V - Topcon Positioning Systems, Inc. [Online]. Available at: https://www.topconpositioning.com/gnss/integrated-gnss-receivers/hiper-v [Accessed: 16 May 2017b].

Trenhaile A. 2002. Rock coasts, with particular emphasis on shore platforms. *Geomorphology* **48**(1–3): 7–22. https://doi.org/10.1016/S0169-555X(02)00173-3.

Trenhaile A. 2016. Rocky coasts – their role as depositional environments. *Earth-Science Reviews* **159**: 1–13. https://doi.org/10.1016/j.earscirev.2016.05.001.

Van Sickle J. 2008. *GPS for Land Surveyors*. CRC Press: New York, NY.

Want R. 2006. An introduction to RFID technology. *IEEE Pervasive Computing* **5**(1): 25–33. https://doi.org/10.1109/MPRV.2006.2.

Wright P, Cross JS, Webber NB. 1978. Aluminium pebbles: a new type of tracer for flint and chert pebble beaches. *Marine Geology* **27**(1–2): 9–17. https://doi.org/10.1016/0025-3227(78)90069-5.

Zingg T. 1935. Beitrag zur Schotteranalyse. *Schweizerische Mineralogische und Petrographische Mitteilungen* **15**: 39–140. https://doi.org/10.3929/ethz-a-000103455.

Supporting Information

Additional supporting information may be found online in the Supporting Information section at the end of the article.

Table A: Bembridge Ledge
Table B: Black Rock
Data S1. Supporting information